Monte Carlo study of a model of diffusion-controlled reactions

Beenakker, C.W.J.; Ross, J.

Citation

Beenakker, C. W. J., & Ross, J. (1986). Monte Carlo study of a model of diffusion-controlled reactions. Retrieved from https://hdl.handle.net/1887/3309

Monte Carlo study of a model of diffusion-controlled reactions

C. W. J. Beenakker[a),b)]
Institute for Theoretical Physics, University of California, Santa Barbara, California 93106
John Ross[c)]
Department of Chemistry, Stanford University, Stanford, California 94305

(Received 25 November 1985; accepted 26 December 1985)

Diffusion-controlled reactions between solute particles and immobile spherical sinks are studied, using the Monte Carlo method to perform averages over sink configurations. The average steady-state solute concentration profile $\bar{c}(r)$ in a locally perturbed solution is determined for sink volume fractions $\phi \leqslant 0.3$, by numerically solving the diffusion equation in the monopolar + dipolar approximation of diffusive couplings between the sinks. At low volume fractions the analytical result $\bar{c}(r) \propto r^{-1} \exp(-r/\lambda)$, with the screening length $\lambda \propto \phi^{-1/2}$, is recovered, whereas for $\phi \gtrsim 0.1$ significant deviations from this functional form are found. The Monte Carlo method is shown to be most accurate and efficient in the region $10^{-3} \lesssim \phi \lesssim 10^{-1}$ in which (a) a system of only 25 sinks suffices, and (b) the monopolar approximation alone is sufficiently accurate. In this regime the reaction rate coefficient calculated numerically is found to be in good agreement with previous analytical theories.

I. INTRODUCTION

The theory of diffusion-controlled reactions, initiated by Smoluchowski,[1] applies to reaction processes in solids and liquids for which mass transport is the rate determining step. In certain situations one of the reacting partners is much larger than the other and may be regarded immobile. This has motivated the extensive study of a model consisting of randomly distributed, immobile, spherical "sinks," which absorb small particles diffusing independently through the solution. For recent reviews of the subject we refer to Refs. 2 and 3.

To analyze this model one has to take into account the competition for solute among the sinks. Because of the long range of diffusive coupling, this competition forms a complicated many-body problem even at low sink concentrations. Exact results are available for the low-density expansion of the effective reaction rate coefficient.[4–6] For more concentrated systems, so-called effective medium theories have been developed[7,8]; no rigorous results are known.[9]

In this paper we examine an altogether different approach to the problem, based on the Monte Carlo method for performing statistical averages[10]: random configurations of nonoverlapping sinks are generated, and for each configuration the steady-state solute concentration field is determined numerically (in an approximation discussed below), under the assumption of perfectly absorbing sinks and an external point source of solute. The average concentration profile $\bar{c}(r)$ is then directly related to the effective transport coefficients studied by previous authors[4–8]; moreover, it contains additional information not obtained previously (the "nonlocal" contributions to the effective transport equation discussed in Ref. 12). The emphasis in this investigation is on the spatial dependence of steady-state concentration fields. Time dependent effects in the case of spatially uniform fields have been studied recently by Fixman,[11] using a related technique.

To calculate the concentration field for a given sink configuration, the time-independent diffusion equation is first transformed to an infinite hierarchy of linear *algebraic* equations for multipole moments of source densities induced on the surfaces of the sinks.[13] A truncation of the hierarchy is then solved numerically. At the lowest level of approximation only the monopolar moments of the induced sources are retained. The resulting simple equations contain the essential features of the problem, in particular the "screening" effect. These same equations have previously been the starting point of computer simulations of the coarsening (Ostwald ripening) of precipitated solutions by Weins and Cahn,[14] and Voorhees and Glicksman.[15] To investigate the accuracy of the monopolar approximation we also study one higher level of truncation, at which both monopolar and dipolar couplings contribute.

The outline of this paper is as follows. In Sec. II we define and discuss the model, and give the formal solution which will form the basis of the numerical calculations. These calculations are the subject of Sec. III. A discussion of the results and comparison with previous analytical work follows in Sec. IV, together with an evaluation of the merits and limitations of the present numerical method.

II. DESCRIPTION OF THE MODEL

We consider a model of diffusion-controlled reactions[3] in which small solute particles are absorbed by immobile spherical sinks. In a steady-state situation the solute molar concentration field $c(\mathbf{r})$ satisfies the time-independent diffusion equation

---

[a)] Work supported in part by the National Science Foundation under Grant No. PHY82-17853, and supplemented by funds from the National Aeronautics and Space Administration.

[b)] Present address: Philips Research Laboratories, P.O. Box 80000, Eindhoven 5600 JA, The Netherlands.

[c)] Work supported in part by the National Science Foundation and the Air Force Office of Scientific Research.

$$D\nabla^2 c(\mathbf{r}) + q^{\mathrm{ext}}(\mathbf{r}) + \Sigma_{i=1}^{N} q_i^{\mathrm{ind}}(\mathbf{r}) = 0, \tag{1}$$

with D the diffusion coefficient in the solvent, an external source density field q^{ext}, and for each of N sinks an induced source density q^{ind} located in its interior. These induced sources are to be chosen in such a way that the solute concentration is zero within the sinks,

$$c(\mathbf{r}) = 0 \quad \text{for } |\mathbf{r} - \mathbf{R}_i| \leqslant a \quad (i = 1,2,\ldots,N), \tag{2}$$

where $\mathbf{R}_i$ denotes the position of the center of sink i and a its radius. (For simplicity, we assume perfectly absorbing and equal-sized sinks; for extensions to more general cases, see Appendix A and Ref. 16.)

This model, and its variants, applies to a wide range of physical and chemical phenomena. One application, to which we shall return, is in the late stage of precipitation from supersaturated solutions (Ostwald ripening).[17] In this connection the field $c(\mathbf{r})$ can be interpreted as the local supersaturation in a solution with a monodisperse array of large precipitated grains and an external source of solute. (Since in this case the grains grow or dissolve in time we are, strictly speaking, not in a steady-state situation; nevertheless, a "quasi-static" approximation holds, provided the external source strength is sufficiently small. The criterion for the validity of this approximation in the case of a point source of strength q_0 is $|q_0| \ll aDv^{-1}\phi^{1/2}$, with v the molar volume of the precipitate and ϕ its volume fraction.[18])

For every given configuration $\{\mathbf{R}^N\}$ of the sinks the concentration field $c(\mathbf{r})$ depends linearly on the external sources through a relation of the form

$$c(\mathbf{r}) = \int d\mathbf{r}'\, m(\mathbf{r},\mathbf{r}';\{\mathbf{R}^N\})\, q^{\mathrm{ext}}(\mathbf{r}'). \tag{3}$$

By using, in the numerical computations, a *point source* of the form $q^{\mathrm{ext}}(\mathbf{r}) = q_0\delta(\mathbf{r})$ we can obtain, therefore, the *microscopic transport kernel m* directly from the concentration field.

To obtain macroscopic quantities we average over the configurations of the sinks. In some situations of interest the positions of the sinks are *correlated* with the location of the external sources. If this is the case (for example, if sinks and sources may not overlap), there is of course no linear relation between *average* concentration and external source field. Such a relation does exist in the case of *uncorrelated* sources and sinks; upon averaging Eq. (3) with a distribution function $P(\{\mathbf{R}^N\})$ which is zero if any pair of sinks overlap and a constant elsewise, we have for the average concentration $\bar{c}(\mathbf{r})$ the equation

$$\bar{c}(\mathbf{r}) = \int d\mathbf{r}'\, M(|\mathbf{r}' - \mathbf{r}|) q^{\mathrm{ext}}(\mathbf{r}'). \tag{4}$$

The *macroscopic transport kernel M* is the average of m in Eq. (3) and depends only on the separation $|\mathbf{r}' - \mathbf{r}|$ because of translational invariance and isotropy.

The (effective) rate coefficient of the reactions k can be defined by

$$k \equiv \Big(\int d\mathbf{r}\, q^{\mathrm{ext}}(\mathbf{r})\Big)\Big(\int d\mathbf{r}\, \bar{c}(\mathbf{r})\Big)^{-1} = \Big(\int d\mathbf{r}\, M(r)\Big)^{-1}. \tag{5}$$

Alternatively, we may define the reaction rate coefficient in terms of the average of the *reduced* source density $q_{\mathrm{red}}^{\mathrm{ext}}$,

$$q_{\mathrm{red}}^{\mathrm{ext}}(\mathbf{r}) = \begin{cases} 0 & \text{if } |\mathbf{r} - \mathbf{R}_i| \leqslant a \text{ for some } i, \\ q^{\mathrm{ext}}(\mathbf{r}) & \text{elsewise,} \end{cases} \tag{6}$$

which is nonzero outside the sinks only. This alternative rate coefficient k_1 is defined by

$$k_1 \equiv \Big(\int d\mathbf{r}\, \overline{q_{\mathrm{red}}^{\mathrm{ext}}}(\mathbf{r})\Big)\Big(\int d\mathbf{r}\, \bar{c}(\mathbf{r})\Big)^{-1} = (1 - \phi)k, \tag{7}$$

and is related to the coeffiicient in Eq. (5) by a factor $(1 - \phi)$, where $\phi = \frac{4}{3}\pi a^3 N/V$ is the volume fraction of the sinks (V is the total volume of the solution). Both definitions (5) and (7) are used in the literature (cf. the discussion in Ref. 19). The reciprocal of k_1 represents the mean time a particle created outside a sink can diffuse before being absorbed, whereas k contains additional contributions from hypothetical particles created inside a sink which are then instantaneously absorbed.

We conclude this section by giving a *formal* solution of Eqs. (1) and (2), which forms the starting point of our numerical calculations. The method used to arrive at this solution is described in Appendix A.[13] Here we shall consider only the case of an external point source $q^{\mathrm{ext}}(\mathbf{r}) = q_0\delta(\mathbf{r})$ at the origin of our coordinate system (see, however, Appendix A). We assume that no sink overlaps the origin. The induced sources $q_i^{\mathrm{ind}}(\mathbf{r})$ are then nonzero on the surfaces of the sinks only and can be expanded into so-called irreducible surface multipole moments $\mathbf{q}_i^{(m)}$. These are constant tensors of rank m which are traceless and symmetric in any pair of their indices. In terms of these moments the formal solution for the concentration field $c(\mathbf{r})$ at any point $\mathbf{r}$ outside the sinks has the form

$$4\pi Dc(\mathbf{r}) = |\mathbf{r}|^{-1}q^0 + \sum_{j=1}^{N}\sum_{m=0}^{\infty}(2m-1)!!a^m \times |\mathbf{r} - \mathbf{R}_j|^{-2m-1}\, \overline{(\mathbf{r} - \mathbf{R}_j)^m} \odot \mathbf{q}_j^{(m)}, \tag{8}$$

where the multipole moments $\mathbf{q}_j^{(m)}$ have to be determined from the following hierarchy of linear algebraic equations:

$$\begin{aligned} n!(2n-1)!!\mathbf{q}_i^{(n)} &+ \sum_{j\neq i}\sum_{m=0}^{\infty}(-1)^m(2n+2m-1)!!a^{n+m+1} \\ &\times |\mathbf{R}_j - \mathbf{R}_i|^{-2n-2m-1}\, \overline{(\mathbf{R}_j - \mathbf{R}_i)^{n+m}} \odot \mathbf{q}_j^{(m)} \\ &= (-1)^{n+1}(2n-1)!!a^{n+1}|\mathbf{R}_i|^{-2n-1}\, \overline{\mathbf{R}_i^n}\, q_0, \\ &(i = 1,2,\ldots,N;\ n = 0,1,2,\ldots). \end{aligned} \tag{9}$$

The double factorial used in these equations is defined by $(2n-1)!! = 1\cdot 3\cdot 5\cdots(2n-3)\cdot(2\mathrm{n}-1)$, with the convention $(-1)!! \equiv 1$ (also, $0! \equiv 1$). The notation $\overline{\mathbf{r}^m}$ denotes an irreducible (traceless and symmetric) tensor of rank m, constructed from the m-fold ordered product of the vector $\mathbf{r}$. For $m = 1,2$ one has, e.g.,

$$\overline{\mathbf{r}} = \mathbf{r}, \quad \overline{\mathbf{r}^2} = \mathbf{r}\mathbf{r} - \tfrac{1}{3}|\mathbf{r}|^2\mathbf{1}, \tag{10}$$

where $\mathbf{1}$ is the second rank unit tensor. Finally, the notation $\odot\, \mathbf{q}^{(m)}$ indicates a full contraction with the multipole moment, e.g.,

$$\overline{\mathbf{r}^m} \odot \mathbf{q}^{(m)} = \sum_{\alpha_1}\cdots\sum_{\alpha_m}(\overline{\mathbf{r}^m})_{\alpha_1\cdots\alpha_m}(\mathbf{q}^{(m)})_{\alpha_m\cdots\alpha_1}, \tag{11}$$

with the convention $\overline{\mathbf{r}^0} \odot q^{(0)} \equiv q^{(0)}$.

III. MONTE CARLO CALCULATIONS

Our numerical computation of the average concentration $\bar{c}(r)$ at a distance r from a point source proceeds as follows.

First, a random configuration of $N = 25$ or $N = 100$ spherical sinks of radius a inside a given volume is generated [using a method discussed in point (5) below]. The configuration is such that (i) no two sinks overlap, (ii) no sink overlaps with the point source, and (iii) no sink overlaps with the point $\mathbf{r}$ at which we are calculating the concentration. At the lowest volume fractions $\phi \leqslant 10^{-2}$ we position the sinks completely inside a spherical container of radius $a(N/\phi)^{1/3}$. The external point source $q^{\text{ext}}(\mathbf{r}) = q_0\delta(\mathbf{r})$ is located at the center of the container (which is also the origin of our coordinate system). At higher volume fractions, however, we choose a cubic volume with "periodic boundary conditions," in order to minimize the effect of container walls on the distribution of configurations. (In this case the external source sits at the center of the cube and the concentration is calculated at points on a line extending from the source to the center of one of the sides of the cube.)

Once a configuration has been generated, a *truncation* of the infinite hierarchy of linear equations (9) is solved numerically[20] for the induced source multipole moments $\mathbf{q}_i^{(m)}$ $(i = 1,2,...,N)$. We use either truncations at the *monopolar* level (i.e., putting $\mathbf{q}^{(m)} \equiv 0$ for $m \geqslant 1$ and solving the equations with $n = 0$ for $q^{(0)}$) or at the *dipolar* level (put $\mathbf{q}^{(m)} \equiv 0$ for $m \geqslant 2$ and find $q^{(0)}$ and $\mathbf{q}^{(1)}$ from the equations with $n = 0$ and 1). The number of equations and unknowns then equals N at the monopolar level or $4N$ at the dipolar level of approximation. Upon substitution of the solution into Eq. (8), we obtain the corresponding approximation of the concentration $c(\mathbf{r})$.

This procedure is repeated for 100 configurations and both the average and the variance of the concentration at the initially determined point $\mathbf{r}$ are computed. Note that the average performed in this way is a *conditional* average, since we have only considered configurations for which none of the sinks overlap with either the external source at the origin, or the point $\mathbf{r}$. From this conditionally averaged concentration $\bar{c}^{\text{cond}}(\mathbf{r})$ we can obtain the unconditional average $\bar{c}(\mathbf{r})$ by multiplying with the probability that both $\mathbf{r}$ and the origin are not inside any sink [since $c(\mathbf{r}) = 0$ if a sink overlaps with either $\mathbf{r}$ or the origin]. This may be written

$$\bar{c}(\mathbf{r}) = (1-\phi)[1-\phi(\mathbf{r})]\,\bar{c}^{\text{cond}}(\mathbf{r}), \tag{12}$$

where $\phi(\mathbf{r})$ is the probability that the point $\mathbf{r}$ lies inside a sink, given that none of the sinks overlap with the origin. This function (which approaches the sink volume fraction ϕ far from both the origin and container walls) is determined to a sufficient accuracy by averaging over 10^4 configurations.

The resulting average concentration profile $\bar{c}(r)$ is shown in Fig. 1 for five volume fractions $\phi = 0.001$, 0.01, 0.1, 0.2, 0.3. For each volume fraction we give the results from the monopolar approximation for both 25 and 100 sinks; the effect of dipolar contributions, however, has been determined for a system of 25 sinks only. The error bars correspond to a statistical uncertainty of plus or minus the standard deviation after averaging over 100 configurations.

We can make the following observations concerning these results.

(1) By comparing the monopolar values for $N = 25$ and $N = 100$ we can assess the influence of *finite-size effects* on the concentration profiles. Quadrupling the number of sinks does not affect the results beyond the statistical uncertainty for $\phi \geqslant 0.1$. At the lowest volume fractions an effect is seen at large r. That the influence of the finite system size should be more pronounced at low rather than high sink concentrations, can be understood by noting that (for given N and a) the range of the concentration profile (i.e., the screening length) scales as $\phi^{-1/2}$, whereas the system size itself increases more slowly with decreasing volume fraction, viz. as $\phi^{-1/3}$. It is a fortunate circumstance that even a very small system of only 25 sinks is already sufficiently large for the present purpose, since the computation time required increases rapidly as N^3 [the solution of the linear equations (9) being the most time-consuming step].

(2) The inclusion of *dipolar contributions* does not have a significant effect for $\phi \leqslant 0.01$. At higher volume fractions, however, these contributions become increasingly important, consistent with the decreasing mean separation of the sinks.

(3) *Screening* of the concentration profile is observed at all volume fractions considered. For $\phi \leqslant 0.01$ a Debye–Hückel profile

$$\bar{c}(r) = \left(\frac{q_0}{4\pi D r}\right)\exp\left(\frac{-r}{\lambda}\right) \tag{13}$$

(corresponding to a straight line through the origin with slope $1/\lambda$ in Fig. 1) fits the data in the range where finite-size effects are insignificant; for $\phi = 0.01$ this is a range of twice the screening length λ. At higher volume fractions, however, deviations from this functional form occur which cannot be attributed to the effect of a finite system size. We find that the concentration decays more rapidly than a Debye–Hückel profile over its entire range.

(4) The *rate coefficient* k of the reactions can be obtained by integrating the concentration profile,

$$k = q_0\left(4\pi\int_0^\infty \bar{c}(r)\,r^2\,dr\right)^{-1}, \tag{14}$$

as follows from Eq. (5). At $\phi = 0.001$ and $\phi = 0.01$ the Debye–Hückel profile (13) fits the data, and we can thus determine the rate coefficient from the screening length λ by $k = D/\lambda^2$. For $\phi \geqslant 0.1$ we calculate k by integrating a cubic spline, fitted to the data points in Fig. 1 and extrapolated linearly outside the range of the data. Since the profile decays rapidly, the contribution to k from the extrapolated tail is small; the length of the error bars in Fig. 2 equals this extrapolated contribution plus the error induced by the statistical uncertainty in the data. The results are discussed in the next section.

(5) Our final point concerns the method adopted to generate random configurations of nonoverlapping sinks. The usual procedure, due to Metropolis *et al.*,[10] is to construct a Markov chain of configurations which have asymp-

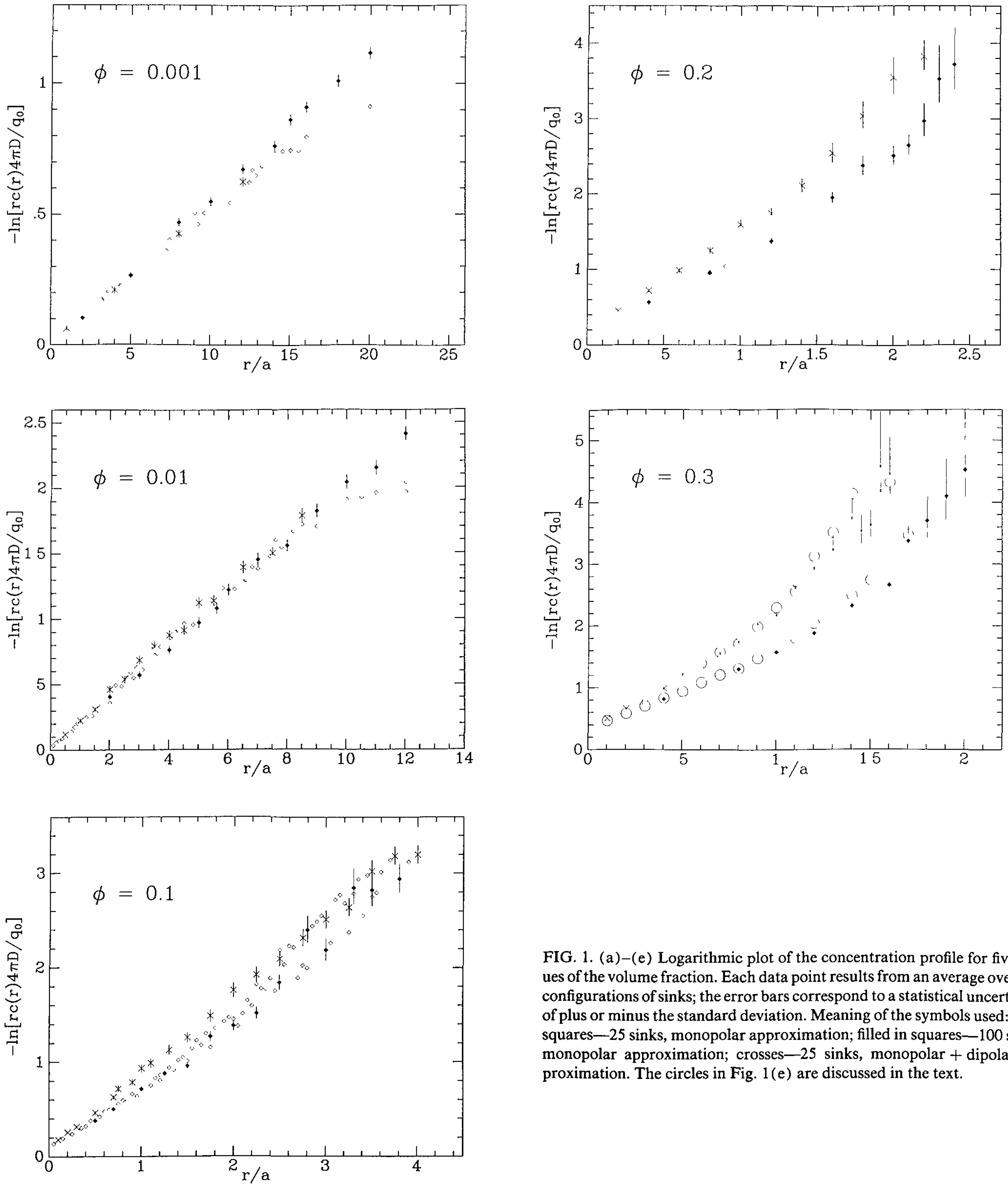

FIG. 1. (a)–(e) Logarithmic plot of the concentration profile for five values of the volume fraction. Each data point results from an average over 100 configurations of sinks; the error bars correspond to a statistical uncertainty of plus or minus the standard deviation. Meaning of the symbols used: open squares—25 sinks, monopolar approximation; filled in squares—100 sinks, monopolar approximation; crosses—25 sinks, monopolar + dipolar approximation. The circles in Fig. 1(e) are discussed in the text.

totically the correct distribution function. In this investigation we chose instead a more efficient *immediate* method, in which one starts with an empty container and then adds sinks one by one to a randomly selected location in the volume which is still available. Although clearly approximate, this latter method is completely satisfactory in the regime of volume fractions $\phi \leqslant 0.3$ considered here. To demonstrate this, we show in Fig. 1(e) also the results obtained at $\phi = 0.3$ using the Metropolis algorithm. These results are indicated by circles, for both the monopolar and monopolar + dipolar approximation in a system of 25 sinks. (In our implementation of the Metropolis algorithm,[10] starting with a configuration obtained by the immediate method described above, we first performed 10^4N one-particle moves in the Markov chain. The maximum step size for each move was such that about 50% of the moves were rejected. Then we made 10^4N more moves, calculating the concentration at every 10^2N configuration.) As one sees in Fig. 1(e), the Metropolis algorithm and the immediate method give fully equivalent results.

IV. DISCUSSION

We have studied diffusion-controlled reactions of small solute particles with immobile spherical sinks, using a method which combines (a) an approximate numerical solution to the time-independent diffusion equation for a given configuration of sinks, with (b) the Monte Carlo technique for performing configurational averages. By calculating the average steady-state solute concentration profile in a solution with an external point source, we have obtained directly the macroscopic transport kernel which relates the concentration field $\bar{c}(\mathbf{r})$ to external sources $q^{\text{ext}}(\mathbf{r})$ [see Eq. (4)].

For a highly dilute system of sinks this relation takes the form

$$-D\nabla^2\bar{c}(\mathbf{r}) + k_0\bar{c}(\mathbf{r}) = q^{\text{ext}}(\mathbf{r}), \tag{15}$$

with D the diffusion coefficient of a solute particle in the solvent and $k_0 = 3\phi D/a^2$ the Smoluchowski rate coefficient (a is the radius of the sinks, and ϕ their volume fraction). A point source $q^{\text{ext}}(\mathbf{r}) = q_0\delta(\mathbf{r})$ then generates a Debye–Hückel profile $\bar{c}(r) = (q_0/4\pi Dr)\exp(-r/\lambda)$, with the screening length $\lambda = (D/k_0)^{1/2}$. These are the well-known mean-field theory results, which are confirmed by our microscopic calculations at very low volume fractions.

In a nondilute system, the concentration field is usually described in the literature[3] by a reaction-diffusion equation of the form (15), but with modified transport coefficients D^{eff} and k (which reduce to, respectively, D and k_0 in the limit $\phi \to 0$). This description has, however, been criticized by Tokuyama and Cukier,[12] who showed on the basis of a formal "scaling expansion" that the *nonlocal* transport equation (4) cannot be reduced to a *local* reaction-diffusion equation by making a small-gradient approximation (except of course in the limit $\phi \to 0$). The point made by these authors is that the transport kernel contains nonlocal contributions which vary on a length scale equal to the range of the diffusive interactions itself (the screening length). Only if the external source is approximately constant over this range does a local description apply, which is then simply given by the rate law

$$k\bar{c}(\mathbf{r}) = q^{\text{ext}}(\mathbf{r}). \tag{16}$$

On a shorter length scale, however, the reaction-diffusion equation contains a nonlocal "diffusion kernel," rather than a simple (effective) diffusion coefficient.

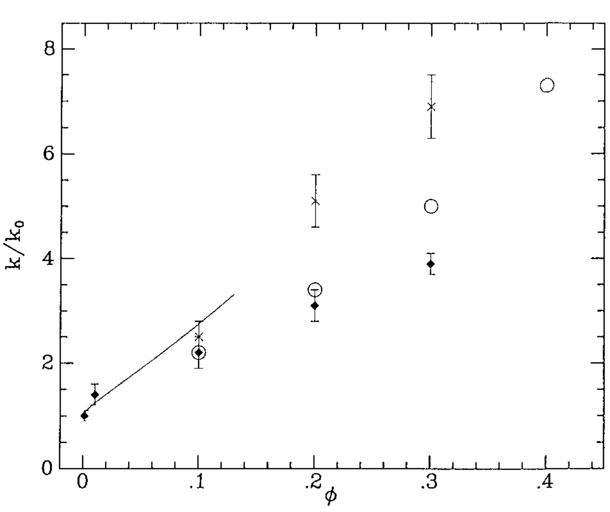

FIG. 2. Rate coefficient k/k_0 vs volume fraction ϕ. Squares—numerical data, monopolar approximation; crosses—numerical data, monopolar + dipolar approximation (coincide with the squares at the two lowest volume fractions); solid curve—low density expansion of Ref. 4; circles—effective medium theory of Ref. 8 [corrected according to Eq. (17)].

The calculations presented in Fig. 1 are, to our knowledge, the first to show this phenomenon explicitly. Deviations from the Debye–Hückel profile (corresponding to a straight line in Fig. 1) are observed over the whole range of the concentration field for volume fractions $\phi \geqslant 0.1$: the field is found to decay more rapidly than the $r^{-1}\exp(-r/\lambda)$ decay which would follow from a local reaction-diffusion equation.

By integrating the concentration field we obtain the reaction rate coefficient k, defined in Eq. (5). Our numerical data are shown in Fig. 2, together with the analytical results from a low-density expansion[4] and an effective medium theory.[8]

At this point it is necessary to mention a difficulty we have encountered in interpreting the effective medium theories as developed by Muthukumar[7] and Cukier and Freed.[8] For technical reasons, these authors assume that solute particles can diffuse freely *inside* the sinks and that the reactions take place only at the sink surfaces. The resulting effective reaction rate k_{EM} will therefore, because of this assumption, be too low in comparison with the rate k in a solution with zero solute concentration inside the sinks. This difficulty is analyzed in Appendix B.[21] It is found that

$$k = k_{EM}\left(1 - \frac{1}{5}\phi^2\frac{k_{EM}}{k_0}\right)^{-1}, \tag{17}$$

where k_0 is the Smoluchowski rate coefficient defined above. The nonlinear transformation (17) turns out to be relatively unimportant in the regime $\phi \leqslant 0.3$ of interest here, although it does substantially change the results of the effective medium theories[7,8] at higher volume fractions (cf. Fig. 3 in Appendix B).

We now return to Fig. 2. At the lowest volume fraction considered, $\phi = 0.001$, we find $k = k_0$ within the statistical uncertainty of the data, in agreement with Smoluchowski's theory.[1] For $\phi \lesssim 0.1$ we also find agreement with the low-density expansion of Felderhof and Deutch,[4] which reads[22]

$$k/k_0 = (1-\phi)^{-1} \times [1 + (3\phi)^{1/2} + 12.71\phi + \tfrac{3}{2}\phi\ln\phi + O(\phi^{3/2}\ln\phi)]. \tag{18}$$

In this regime of volume fractions the dipolar contribution to k is small compared with the monopolar contribution, indicating the accuracy of the monopolar approximation of diffusive couplings. For $\phi > 0.1$, however, dipolar couplings become increasingly important, as is evident from Fig. 2. Note that at $\phi = 0.3$ the inclusion of dipolar contributions almost doubles the reaction rate coefficient. We should therefore expect that interactions of still higher multipolarity will substantially alter our results at these high volume fractions.[23] Also shown in Fig. 2 are high density results from the effective medium theory of Cukier and Freed[8] (which, according to these authors, is an improvement upon that of Muthukumar[7]). Their theory is in agreement with the numerical data for $\phi \lesssim 0.1$, and at higher volume fractions gives results which fall between the data from the monopolar and monopolar + dipolar approximations. It is well possible that better agreement at high densities would be obtained by including more higher order multipoles. In this connection we mention that Fixman has developed an effective medium theory which includes the effects of correlations between pairs of sinks and which gives values for the rate coefficient that are in excellent agreement with the results of his numerical calculations.[11] A direct comparison with the present work is not possible, however, since in the model considered by Fixman solute particles can diffuse from the inside of a sink to the outside (and vice versa)—whereas here we are dealing with perfectly absorbing sinks. We also mention an interesting calculation by Keizer, based on fluctuating nonequilibrium thermodynamics.[24] His result for the reaction rate coefficient is close numerically to the effective medium theories for $\phi \lesssim 0.1$, but then increases very steeply and has a singularity at $\phi = 0.18$. No such behavior is observed here.

The present investigation clearly demonstrates both the merits and limitations of the Monte Carlo method for studying diffusion-controlled reactions. In the regime $10^{-3} \lesssim \phi \lesssim 10^{-1}$ this method forms an efficient and reliable technique which, in contrast to various analytical approaches, can be directly applied to ensembles of reactive sinks with arbitrary statistical properties. We have shown that in this regime of volume fractions (a) a very small system of only 25 sinks suffices, and (b) the monopolar approximation of diffusive couplings is sufficiently accurate. As a result, the necessary computations require little computer time and storage. Both at lower and higher volume fractions, however, the Monte Carlo method becomes increasingly less efficient: (a) for $\phi < 10^{-3}$, a larger system is necessary because of the increasing screening length; (b) for $\phi > 10^{-1}$, contributions from higher order multipoles must be included, as a result of the decreasing separation of the sinks.

We finally note that the volume fraction regime in which the Monte Carlo method is most efficient, is also the regime of interest in recent theoretical studies of Ostwald ripening,[25,26] which aim to determine the effect on the ripening process of dynamical correlations between the positions and sizes of the precipitated particles (sinks). The numerical method discussed in this paper is particularly suitable for that problem.[27]

ACKNOWLEDGMENTS

We thank M. Marder for a valuable discussion. Carlo Beenakker gratefully acknowledges a fellowship from the Niels Stensen Stichting, and wishes to thank the members of the Institute for Theoretical Physics, in particular Professor J. S. Langer, for their hospitality.

APPENDIX A: FORMAL SOLUTION OF THE DIFFUSION EQUATION

In this Appendix the boundary value problem given by Eqs. (1) and (2) is transformed to an infinite hierarchy of linear *algebraic* equations. A truncation of this hierarchy forms the basis of the numerical computations. The present analysis is a direct application to the Poisson equation of the method of induced forces developed for the hydrodynamic Stokes equation. For more details, therefore, we refer to the paper by Mazur and van Saarloos,[13] and to Ref. 28.

It is convenient to first of all Fourier transform the time-independent diffusion equation (1) to

$$-Dk^2 c(\mathbf{k}) + q^{\text{ext}}(\mathbf{k}) + \sum_{j=1}^{N} q_j^{\text{ind}}(\mathbf{k}) = 0, \tag{A1}$$

with the Fourier transform defined by

$$c(\mathbf{k}) = \int d\mathbf{r}\, e^{-i\mathbf{k}\cdot\mathbf{r}} c(\mathbf{r}). \tag{A2}$$

(In this Appendix, k equals $|\mathbf{k}|$ and not the rate coefficient.) The induced sources q_j^{ind} are to be chosen in such a way that

$$c(\mathbf{r}) = 0 \quad \text{for } |\mathbf{r} - \mathbf{R}_j| \leqslant a_j \quad (j = 1,2,\ldots,N), \tag{A3}$$

where a_j is the radius of sink j. We relax here the assumption of equal-sized sinks made in Eq. (2).

Without loss of generality we may assume that the external source field $q^{\text{ext}}(\mathbf{r})$ is zero inside the sinks (since a nonzero contribution in the interior of, say, sink j is canceled by part of q_j^{ind}). The induced sources are then localized entirely on the surfaces of the sinks and may be expanded in irreducible surface multipole moments, defined by

$$\mathbf{q}_j^{(p)} \equiv a_j^{-p} (p!)^{-1} \int d\mathbf{r}\, \overline{(\mathbf{r} - \mathbf{R}_j)^p}\, q_j^{\text{ind}}(\mathbf{r}). \tag{A4}$$

For the Fourier transformed induced source this expansion is given by

$$q_j^{\text{ind}}(\mathbf{k}) = \sum_{p=0}^{\infty} (2p+1)!!(-i)^p j_p(a_j k)\, \overline{\hat{\mathbf{k}}^p} \odot \mathbf{q}_j^{(p)}, \tag{A5}$$

with $\hat{\mathbf{k}} = \mathbf{k}/|\mathbf{k}|$ and j_p the spherical Bessel function of order p. [See also the definitions given directly below Eq. (9).]

To determine the multipole moments of the induced source, we take surface moments of the concentration field. These latter quantities are defined by

$$\overline{\overline{\hat{\mathbf{n}}_j^p} c}^{S_j} \equiv (4\pi a_j^2)^{-1} \oint_{S_j} dS\, \overline{\hat{\mathbf{n}}_j^p}\, c(\mathbf{r}), \tag{A6}$$

where S_j is the surface of sink j, and $\hat{\mathbf{n}}_j$ a unit vector perpendicular to that surface and pointing outwards. Equation (A6) may also be written as

$$\overline{\overline{\hat{\mathbf{n}}_j^p} c}^{S_j} = (2\pi)^{-3} \int d\mathbf{k}\, e^{i\mathbf{k}\cdot\mathbf{R}_j} j_p(a_j k)\, \overline{\hat{\mathbf{k}}^p}\, c(\mathbf{k}). \tag{A7}$$

Because of the boundary condition (A3) we have for each p the identity

$$\overline{\overline{\hat{\mathbf{n}}_j^p} c}^{S_j} = 0 \quad (p = 0,1,2,\ldots). \tag{A8}$$

Combining Eqs. (A1), (A5), (A7), and (A8) we thus obtain the hierarchy of equations

$$\sum_{j=1}^{N}\sum_{l=0}^{\infty}\mathbf{A}_{ij}^{(p,l)}\odot\mathbf{q}_j^{(l)}=-4\pi Da_i(2p+1)!!\,\overline{\overline{\hat{\mathbf{n}}_i^{p}}c_0}^{S_i}$$
$$(i=1,2,\ldots,N;\ p=0,1,2,\ldots).\qquad\text{(A9)}$$

Here the "connector" **A** is defined by

$$\mathbf{A}_{ij}^{(p,l)}=\tfrac{1}{2}\pi^{-2}a_i\,i^{p-l}(2p+1)!!(2l+1)!!\int d\mathbf{k}\,e^{-i\mathbf{k}\cdot\mathbf{R}_{ij}}$$
$$\times k^{-2}j_p(a_ik)\,j_l(a_jk)\,\overline{\hat{\mathbf{k}}^{p}}\,\overline{\hat{\mathbf{k}}^{l}},\qquad\text{(A10)}$$

with $\mathbf{R}_{ij}=\mathbf{R}_j-\mathbf{R}_i$. The right-hand side of Eq. (A9) is a surface moment of the unperturbed concentration field c_0, given by

$$c_0(\mathbf{k})=(Dk^2)^{-1}q^{\text{ext}}(\mathbf{k}).\qquad\text{(A11)}$$

The evaluation of the integral expression (A10) for the connectors proceeds along the same lines as in the hydrodynamic case.[28] We give therefore only the results,

$$\mathbf{A}_{ii}^{(p,l)}\odot\mathbf{q}_i^{(l)}=\delta_{pl}\,p!(2p-1)!!\mathbf{q}_i^{(p)},\qquad\text{(A12)}$$

$$\mathbf{A}_{ij}^{(p,l)}=(-1)^l(2p+2l-1)!!\,a_i^{p+1}a_j^lR_{ij}^{-(2p+2l+1)}\,\overline{\mathbf{R}_{ij}^{p+l}}$$
$$(i\neq j,\quad R_{ij}>a_i+a_j),\qquad\text{(A13)}$$

with $R_{ij}=|\mathbf{R}_{ij}|$. Similarly, for the surface moments of c_0 we have the expression

$$4\pi Da_i(2p+1)!!\;\overline{\overline{\hat{\mathbf{n}}_i^{p}}c_0}^{S_i}=(2p-1)!!a_i^{p+1}$$
$$\times\int d\mathbf{r}|\mathbf{r}-\mathbf{R}_i|^{-(2p+1)}\,\overline{(\mathbf{r}-\mathbf{R}_i)^p}\,q^{\text{ext}}(\mathbf{r}).\qquad\text{(A14)}$$

Substituting Eqs. (A12)–(A14) into Eq. (A9) we obtain the set of equations

$$p!(2p-1)!!\,\mathbf{q}_i^{(p)}+\sum_{j\neq i}\sum_{l=0}^{\infty}(-1)^l(2p+2l-1)!!\,a_i^{p+1}a_j^l$$
$$\times R_{ij}^{-(2p+2l+1)}\,\overline{\mathbf{R}_{ij}^{p+l}}\odot\mathbf{q}_j^{(l)}=-(2p-1)!!a_i^{p+1}$$
$$\times\int d\mathbf{r}|\mathbf{r}-\mathbf{R}_i|^{-(2p+1)}\,\overline{(\mathbf{r}-\mathbf{R}_i)^p}\,q^{\text{ext}}(\mathbf{r})$$
$$(i=1,2,\ldots,N;\ p=0,1,2,\ldots),\qquad\text{(A15)}$$

which formally determine the induced source multipole moments. Once these are known, the concentration field follows from Eqs. (A1) and (A5). At any point outside the sinks we have the formula

$$4\pi Dc(\mathbf{r})=\int d\mathbf{r}'|\mathbf{r}'-\mathbf{r}|^{-1}q^{\text{ext}}(\mathbf{r}')$$
$$+\sum_{j=1}^{N}\sum_{l=0}^{\infty}(-1)^l(2l-1)!!\,a_j^l|\mathbf{R}_j-\mathbf{r}|^{-(2l+1)}$$
$$\times\overline{(\mathbf{R}_j-\mathbf{r})^l}\odot\mathbf{q}_j^{(l)}\quad(|\mathbf{R}_j-\mathbf{r}|>a_j),$$
$$\text{(A16)}$$

which follows upon inverse Fourier transformation of Eq. (A1).

For the special case of an external point source, $q^{\text{ext}}(\mathbf{r})=q_0\delta(\mathbf{r})$, and equal-sized sinks, Eqs. (A15) and (A16) reduce to Eqs. (8) and (9) in Sec. II.

APPENDIX B: CORRECTION OF EFFECTIVE MEDIUM THEORIES

In the effective medium theories of diffusion-controlled reactions developed by Muthukumar[7] and Cukier and Freed,[8] it is assumed for technical reasons that solute particles diffuse freely inside the sinks and react only at the sink surfaces. To apply these theories to a system with perfectly absorbing sinks we must, therefore, correct for the nonzero concentration field in the interior of the sinks. For the effective reaction rate coefficient this correction can be made as follows.

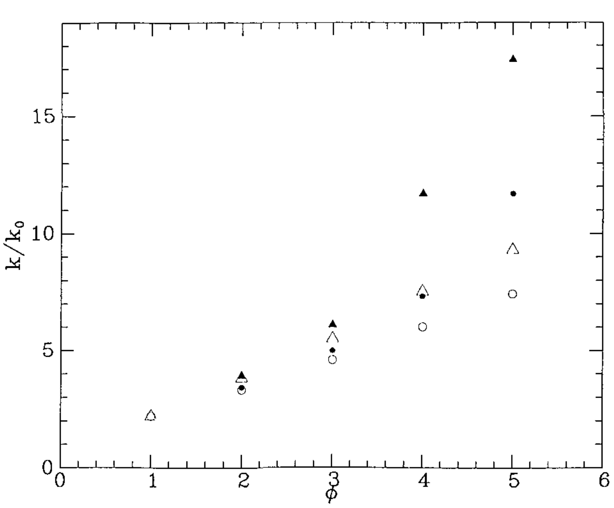

FIG. 3. Rate coefficient k/k_0 vs volume fraction ϕ. Triangles—effective medium theory of Ref. 7; circles—effective medium theory of Ref. 8. The open symbols show the results obtained by these authors, while the filled in symbols are the corrected results according to Eq. (B4). (At the lowest volume fraction all four symbols coincide.)

Since the rate coefficient is, by definition, independent of the external source density field, we may determine it by considering a spatially uniform field $q^{\text{ext}}(\mathbf{r})\equiv q^{\text{ext}}$. If we require, following Refs. 7 and 8, that the concentration field $c(\mathbf{r})$ vanishes only at the surfaces of the sinks, then we have inside each sink the following static solution of the diffusion equation:

$$c(\mathbf{r})=\tfrac{1}{6}(a^2-|\mathbf{r}-\mathbf{R}_i|^2)\frac{q^{\text{ext}}}{D}\quad(|\mathbf{r}-\mathbf{R}_i|\leqslant a,$$
$$i=1,2,\ldots,N).\qquad\text{(B1)}$$

The total number of solute particles inside the sinks per unit volume is then given by

$$\frac{1}{V}\sum_{i=1}^{N}\int_{|\mathbf{r}-\mathbf{R}_i|<a}d\mathbf{r}\,c(\mathbf{r})=\frac{1}{15}\phi q^{\text{ext}}\frac{a^2}{D}.\qquad\text{(B2)}$$

The reciprocal rate (or mean particle lifetime) k_{EM}^{-1} in the effective medium theories is therefore too large by the amount $\frac{1}{15}\phi(a^2/D)$, when compared with the reciprocal rate k^{-1} for perfectly absorbing sinks [defined in Eq. (5)],

$$k^{-1}=k_{EM}^{-1}-\frac{1}{15}\phi\frac{a^2}{D}.\qquad\text{(B3)}$$

Equation (B3) may be rewritten as

$$\frac{k}{k_0}=\frac{k_{EM}}{k_0}\left(1-\frac{1}{5}\phi^2\frac{k_{EM}}{k_0}\right)^{-1}.\qquad\text{(B4)}$$

In Fig. 3 we show the effect of the correction (B4) on the results of Refs. 7 and 8. It is relatively unimportant for $\phi\lesssim 0.3$, but substantially affects the results of these papers at higher volume fractions.

[1] M Smoluchowski, Phys Z **17**, 557,585 (1916), Z Phys Chem (Leipzig) **92**, 129 (1917)

[2] A D Brailsford and R Bullough, Philos Trans R Soc London Sect A **302**, 87 (1981)

[3] D F Calef and J M Deutch, Annu Rev Phys Chem **34**, 493 (1983)

[4] B U Felderhof and J M Deutch, J Chem Phys **64**, 4551 (1976)

[5] A D Brailsford, J Nucl Mater **60**, 257 (1976)

[6] J R Lebenhaft and R Kapral, J Stat Phys **20**, 25 (1979)

[7] M Muthukumar, J Chem Phys **76**, 2667 (1982)

[8] R I Cukier and K F Freed, J Chem Phys **78**, 2573 (1983)

[9] At least not for randomly distributed sinks However, exact results for a regular array of sinks have been derived by B U Felderhof, Physica A **130**, 34 (1985)

[10] N A Metropolis, A W Rosenbluth, M N Rosenbluth, A H Teller, and E Teller, J Chem Phys **21**, 1087 (1953)

[11] M Fixman, J Chem Phys **81**, 3666 (1984)

[12] M Tokuyama and R I Cukier, J Chem Phys **76**, 6202 (1982)

[13] The formalism used is an adaptation of the "method of induced forces" employed in the context of a hydrodynamic boundary-value problem by P Mazur and W van Saarloos, Physica A **115**, 21 (1982)

[14] J J Weins and J W Cahn, in *Sintering and Related Phenomena*, edited by G C Kuczynski (Plenum, New York, 1973)

[15] P W Voorhees and M E Glicksman, Acta Metall **32**, 2001, 2013 (1984)

[16] M Muthukumar and R I Cukier, J Stat Phys **26**, 453 (1981)

[17] P W Voorhees, J Stat Phys **38**, 231 (1985)

[18] To arrive at this estimate, we require the characteristic relaxation time λ^2/D of the diffusive fields (with screening length λ) to be much smaller than the time in which the volume of a precipitated particle changes by an appreciable fraction Since there are approximately $\phi(\lambda/a)^3$ particles within a screening length of the point source, this latter time is of order $a^3\phi(\lambda/a)^3(v|q_0|)^{-1}$ The final estimate $\lambda \sim a/\sqrt{\phi}$ (see Sec IV) yields the criterion given in the text

[19] B U Felderhof, J M Deutch, and U M Titulaer, J Chem Phys **76**, 4178 (1982)

[20] All computations were performed on a VAX-11/750 computer, using numerical routines from the PORT library (Bell Laboratories)

[21] This difficulty should not be confused with the point raised in Ref 19 concerning the distinction between the rate coefficient k defined in Eq (5), and the coefficient k_1, defined in Eq (7) in terms of the "reduced" source density These two coefficients are related simply by $k_1 = (1-\phi)k$

[22] The factor $(1-\phi)^{-1}$ in Eq (18) appears because the expansion in Ref 4 is for the quantity $k_1 = (1-\phi)k$, rather than for k

[23] For this reason, the results of the computer simulation of Ostwald ripening by Voorhees and Glicksman (Ref 15) (based on the monopolar approximation) are quantitatively unreliable in the regime $\phi > 0$ 1

[24] J Keizer, J Phys Chem **85**, 940 (1981), J Chem Phys **79**, 4877 (1983) These papers also contain an interesting analysis of correlations between fluctuations in the concentration of the diffusing solute particles

[25] M Tokuyama and K Kawasaki, Physica A **123**, 386 (1984), M Tokuyama, K Kawasaki, and Y Enomoto (preprint)

[26] M Marder, Phys Rev Lett **55**, 2953 (1985)

[27] C W J Beenakker, Phys Rev A (submitted)

[28] C W J Beenakker, W van Saarloos, and P Mazur, Physica A **127**, 451 (1984)